Study of Metallic Nanoshelled Structures with Rigorous Electromagnetic Analysis

Xudong Cui [a *], Daniel Erni [a *],
Christian Hafner [b], Kakhaber Tavzarashvili [b], Ruediger Vahldieck [b]

[a] General and Theoretical Electrical Engineering (ATE), Faculty of Engineering, University of Duisburg-Essen, D-47048 Duisburg, Germany.
[b] Laboratory for Electromagnetic Fields and Microwave Electronics, ETH Zurich, CH-8092, Zurich, Switzerland.

ABSTRACT

The main goal of this paper is to present thorough investigations for the metallic nanoshelled structures with rigorous electromagnetic analysis. Two metallic nanoshelled structures are investigated; namely, single nano-shelled cylinder, and nano-shelled photonic crystals. A rigorous Maxwell's equations solver is used to get insights into the optical properties of the structures. Our numerical simulations show that it is difficult to shift the plasmon resonance to long wavelength (e.g. towards ten micrometers) in such a structure. Flat bands are found in the metallic nanoshelled photonic crystals when the lattice constants are much smaller than the operating wavelength. This would become interesting especially for realizing ultra-compact slow wave structures such as plasmonic devices with low group velocity. Several applications using nano-shelled particles as sensors, as substrates for surface enhanced Raman spectroscopy are also discussed in the paper.

Keywords: Surface plasmon resonances, nano-shelled structure, metallic photonic crystals, numerical simulations

I. INTRODUCTION

Metal nanoparticles offer an advantage over other systems because their optical constants resemble those of the bulk metal to exceedingly small dimensions [1]. Because of this, it is believed that metallic nanoparticles are prone to become building blocks of future new optoelectronic devices [2], followed by the requirements of miniaturization of devices. Among those metal nanoparticles, metallic nanoshelled structures are of particular interest due to their wide tunable ranges of surface plasmon resonances, resulting in applications such as surface plasmon resonance sensing [3, 4, 5, 6], surface enhanced Raman scattering (SERS) [5, 7, 8, 9, 10], Tip-Enhanced Raman Scattering (TERS) [11] and novel plasmonic devices [12, 13, 14]. Moreover, the plasmonic properties allow for the development of fundamentally new metal-based sub-wavelength optical elements [e.g., mirrors, beam-splitters, interferometers, plasmon-enhanced LED etc.] with great potential [11, 15]. Now, with the development of modern nano-fabrication technology, metallic nano-shelled structures can be easily synthesized and chemically modified.

* xudong.cui@uni-duisburg-essen.de, daniel.erni@uni-duisburg-essen.de

Optomechatronic Micro/Nano Devices and Components III, edited by Lixin Dong, Yoshitada Katagiri, Eiji Higurashi, Hiroshi Toshiyoshi, Yves-Alain Peter, Proceedings of SPIE Vol. 6717, 67170O, (2007)
0277-786X/07/$18 · doi: 10.1117/12.754349

Since the dimensions of nanoparticles are typically at the order of nanometers, the ratio of the surface area to the associated particle volume become much larger than their bulk counterparts. As a consequence, the physical and chemical properties of the structures can be dramatically changed. Therefore, the surface effect and volume effect then become more prominent and important for nanoparticles. In order to implement functionality in such nanoscale dimensions, one must take all these effects into account when modeling the structural behavior of nanoparticles.

Currently, theoretical studies on metallic nanoshelled structures are focusing on the linear optical properties [16] and numerous experiments have already been carried out [17]. Despite the large empirical basis, the challenge of numerical simulation is still present because of the limitations of the computational methods and the available computer sources. The applications [i.e., plasmon resonance sensing, SERS etc.] shown above are very sensitive to the electromagnetic fields at or near the particle surfaces, thus providing new challenges to the development of accurate numerical methods. In this work, we focus on the nanostructure formed by the metallic shell with a cylindrical dielectric core confined within a host medium. We then calculated the extinction spectra of the structure using a rigorous two-dimensional (2D) Maxwell's equations solver. The tunability of plasmon resonances is studied and a promising structure made by nanoshelled rods is proposed here, in the framework of a metallic nanoshelled photonic crystals. This work shows that the plasma frequencies can be extensively engineered when using shelled structures within a dielectric host. We also consider in particular via numerical simulations how the plasma frequencies can be shifted. This is demonstrated along the most demanding part of this work namely the computation of the full band diagram for the metallic photonic crystal structures are also given.

II. NUMERICAL METHODS

Although the large number of methodologies available for solving Maxwell's equations, there are, however, some important challenges associated with metal nanoparticles that limit the applicability of methods used to study problems with much longer wavelengths than the structural length scales. Briefly speaking, for nanoparticles, Maxwell's equations are no longer invariant to scaling of both the wavelength and structure size, because of the large material dispersion that is even emphasized in the framework of such small particle dimensions.

For the nanoshelled structures with high symmetry (i.e., for spherical structures), Mie's theory can provide comprehensive analytical descriptions of both of near field and far field behaviors [18]. As soon as the structural symmetry is reduced, it is no longer possible to obtain closed-form solutions to Maxwell's equations. Therefore, a great deal of effort has been put into the development of numerical methods in order to tackle metallic nanostructures. Some representative methods are the Discrete Dipole Approximation (DDA) [19], the Multiple Multipole methods (MMP) [20], and other more general electromagnetic field solvers like the Finite Difference Time Domain (FDTD) [21] and the Finite Element Methods (FEM) [22].

The MMP method that has been used throughout our work is based on Mie-Vekua theory [23], which is essentially close to the analytic solutions to Maxwell's equations. When dealing with nanoparticles, the particle is divided into domains with shapes that allow for series expansion solutions of Maxwell's equations. The coefficients in these expansions are then determined by matching boundary conditions at the domain interface, where the least squares are used for minimizing the matching errors at the boundary. So the resulting solutions are exact within each domain but approximate at the boundaries. One important issue here is that the material parameters for small nanoparticles (i.e., less than 5nm) need to be modified in order to correctly model the size and boundary effect. Usually, the optical dispersion of metal can

be described by a simple Drude model

$$\varepsilon(\omega) = \varepsilon_0[1 - \frac{\omega_p^2}{\omega(\omega + i\gamma)}] \quad (1)$$

Where ε_0 is the permittivity of free space, and ω_p is the plasma frequency of metal, γ is the damping frequency. However, we have to note that this Drude model shown in (1) was valid for bulk materials when the interband transition effects and dephasing due to electron surface scattering can be neglected. For small particles, these effects are revealed by the damping factor γ with a term dependent on the local plasmon-system geometry [24].

$$\gamma_f = \gamma + 2v_f / d \quad (2)$$

γ_f is the modified damping frequency for small particle; v_f is the Fermi velocity [25] and d is the particle diameter. In some cases, in order to describe an intraband transition, the Lorentz oscillator model was used [26]. More precise dielectric models can be obtained through combining Drude and Lorentz model by considering the dielectric response when it is above the threshold of the resonant interband electronic transitions [18]. Finally, the dielectric function for the metal is obtained by fitting the combined Drude model in equation (1) and (2) to the experimental data reported by Johnson and Christy [27] on bulk metal. A more sophisticated approach to fit the measured data to the Drude-like model can be found in [28], where a symbolic regression procedure iterated with the generalized genetic programming was employed and without taking care of further physical limitations.

III. SIMULATION RESULTS AND DISCUSSION

In this simulation work, we focus on two structures: the nanoshelled cylinder, and the metallic nanoshelled photonic crystal. Corresponding properties are also partially investigated in the following subsections.

3.1 Nanoshelled cylinder

The first structure we consider here is the single nanoshell cylinder, which consists of a cylindrical dielectric core with radius r_1 and a metallic shell with radius r_2 in a suspending medium with the permittivity ε_0. The permittivity of the dielectric core is ε_1 and the complex permittivity of the metallic shell is ε_2. The electric field distribution in each of the three regions could be obtained analytically within the electrostatic approximation by the solution of Laplace's equation with the corresponding boundary conditions [2]. It is well known from analytical expressions that the fields in the core, shell and suspending medium are position dependent and the resonances are governed by the combination of the material dispersion and the geometrical parameters. Study shows that the resonances in metallic shelled structures have a much larger tuning range than the metallic core model [26]. We are thus investigating the resonances in the structure.

In the nanoshelled cylindrical structure, the resonance can be tuned by adjusting the shell thickness $\Delta r = r_2 - r_1$, the material parameters ε_1, ε_2, ε_3 simultaneously or just simply changing one of the parameters at one time. The resonance frequencies can be obtained numerically by calculating either the absorption, the scattering cross section or – as shown e.g. in Figure 1 – the extinction efficiency of the structure over the frequency range of interest. The frequencies corresponding to the peak values in the obtained curves are assigned as the resonance frequencies labeling a resonance condition where the electric field on the particle's surface is strongly enhanced.

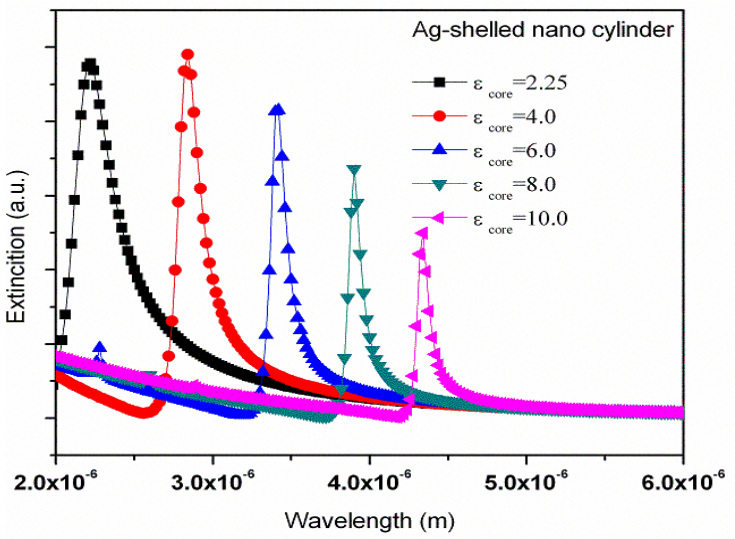

(a)

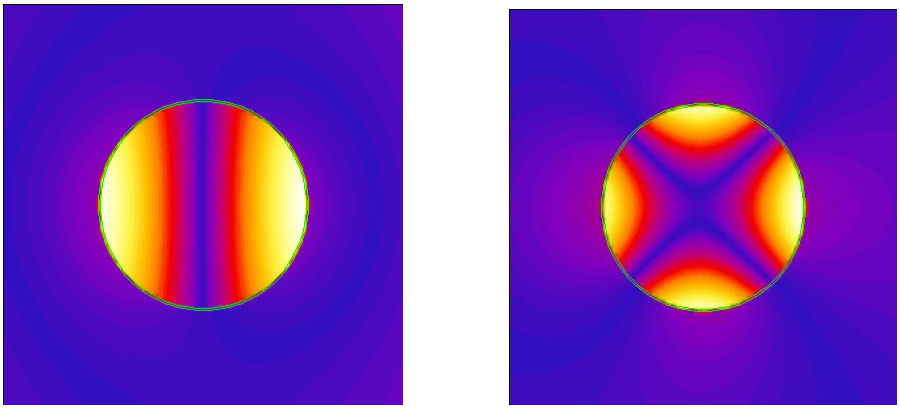

(b) (c)

Fig.1: (a) Calculated plasmon resonance spectra for different core materials on a silver shell of 4.5nm thickness; (b) H-field distribution at the wavelength of 3.42μm (showing the aforementioned dipole nature) and (c) H-field distribution at the wavelength of 2.28μm (showing the aforementioned multipole nature) when the permittivity of the core material is 6.0. Note that the bright color in the figures (b) and (c) indicates high field values.

To get a first impression of the material selection, we calculated the extinction spectra of the structure with different dielectric core materials, while the geometry parameters r_1, r_2 are fixed. Figure 1 shows the calculated plasmon resonance spectra for particles with silver coating and different core materials. The radius of the core r_1 is 258 nm and the thickness of the shell is 4.5 nm (r_2 = 262.5 nm). As depicted in Figure 1 (a) the plasmon resonance is red-shifted when the permittivity of the dielectric core is increased, while the quality factor of the resonance peak decreases. There are two or even more resonance peaks within the wavelength range of interest. It is believed that these peaks originate from different orders, such as dipole or multipoles resonances. We then checked the field distributions associated to the

corresponding resonances: At short wavelength, a multipole behavior is clearly observed; while at long wavelength, the dipole behavior is dominant, as shown in Fig. 1(b) and Fig. 1(c). This can be explained by the fact that a nanoparticle, which is much smaller than the wavelength will at first respond as a dipole to the impinging optical field [29]. More complex distributions arise then from the interplay between the light field and the plasmonic material response.

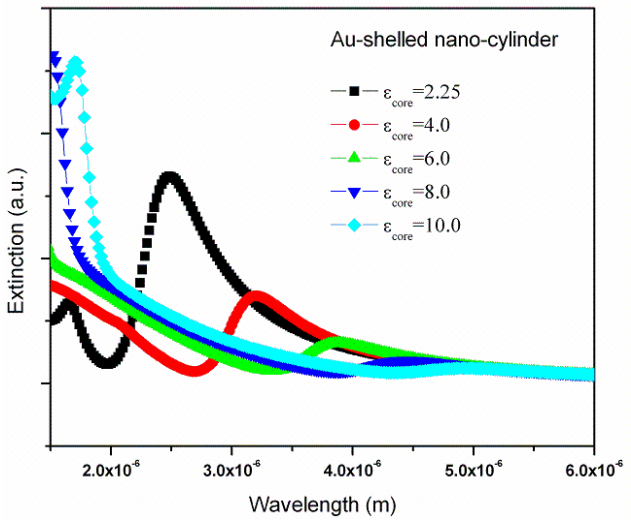

Fig.2: Calculated plasmon resonance spectra for different core materials for a gold shell of 4.5nm thickness.

Among the noble metals, silver is best known to have one amongst the shortest plasma wavelengths [27]. Typically, the plasmon wavelength for silver particle is in ultraviolet therefore it is often used for short wavelength operation like SERS in blue light region at 488nm [11]. While in some occasions, i.e., the SERS application in red or near infrared, the metal with longer plasma wavelength (like gold) is preferred. In Figure 2 the resonance behavior is shown for a gold-coated nanocylinder with the same core material. The resonance becomes broader and the quality factor is lower than those of silver indicating a larger absorption in the particle. Moreover, the resonance peak even becomes almost indistinguishable when the core material exhibits a large permittivity. Unfortunately this also holds for long wavelengths when the core material has a significantly lower permittivity, unveiling the structural limitations of the device when a long wavelength plasmon resonance is desired.

Besides the material properties of the shell and the core, the thickness of the metallic shell is another crucial factor that determines the optical properties of the structures. The plasma resonance is red shifted with the decreasing shell thickness (at fixed the core materials and diameters). Surprisingly, the plasmon resonance can be tuned to extraordinary large wavelengths up to 7.5μm while the shell thickness is approaching a value of 0.3nm as shown in Figure 3. This is to our best knowledge the largest wavelength ever predicted numerically for metallic optical nanocylinders so far. A further study shows that when the material properties are fixed, the resonance wavelength mainly depends on the core/shell ratio $r_1/\Delta r$, where the resonance wavelength grows with the increasing core/shell ratio. This is also in accordance with the theoretical predictions for gold-shelled spherical nanoparticles [17].

It is worth noting that all these materials usually exhibit complex permittivities, leading resonance conditions for the overall structure which are more complicate to retrieve. Since the metallic part still plays important roles on the optical

response, the general design rules still hold for nano-shelled cylinders. Structures with nonlinear material properties define an interesting topic of its own and will certainly merit some future research.

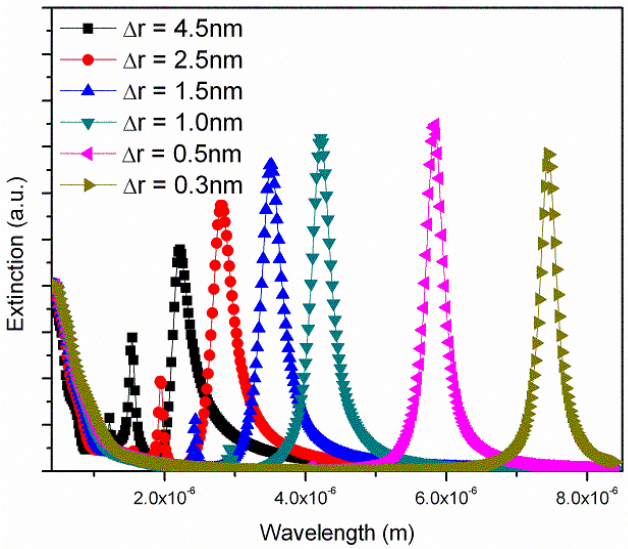

Fig.3: Calculated plasmon resonance spectra for different Ag shell thicknesses.

3.2 Photonic crystals with metal-shelled cylinders

Photonic crystals (PhCs) are artificial materials, which consist of at least two materials exhibiting a high index contrast that are periodically arranged on certain lattices. Because of the periodicity of the structure, the electromagnetic wave is modulated within such structures, resulting in new optical phenomena based on the presence of a photonic band gap (PBG) [30]. What makes PhCs most attractive in optics is the fact that no light may penetrate a PhC at wavelengths within the PBG. For metallic photonic crystals (MPhCs), novel applications have been found to form negative index materials at radio frequencies [31] and to enhance the nonlinear optical properties at optical frequencies [32]. In particular, the emergence of flat bands in the MPhC's band diagram and tackling these operating frequencies by efficient numerical methods are of particular interest because slow wave phenomena may become crucial in the context of both functionality and integration density for future nanophotonic devices.

Referring to the wide tuning range of the resonance wavelengths in the metal–shelled structure, we will study its impact on the band diagram of the MPhCs made of metallic shelled cylinders. To observe the surface plasmon resonance behaviors in MPhCs, certain configurations should be adopted, i.e., the H-polarization has to be used where the magnetic field is parallel to the axis of the cylinders. The metallic nanoshelled cylinders are arranged on a 2D square lattice with lattice constant a =750 nm and the background material is air. For the nanoshelled cylinder, the radius of the core r_1 is 225nm, and the shell thickness is 37.5nm (r_1/a = 0.30, r_2/a = 0.35). Figure 4 shows the calculated band diagram for the MPhC structure. In accordance with our previous research [33, 34], there are no flat bands appear in the PBG when silver is used as coating material. To a first intention one may question the calculations because previous numerical investigations had already demonstrated the existence of flat bands in such MPhC structures [35]. The fact is that mostly

idealized models for metals are used reproducing unrealistic low loss figures, which does not agree with the measured data for metallic materials [35].

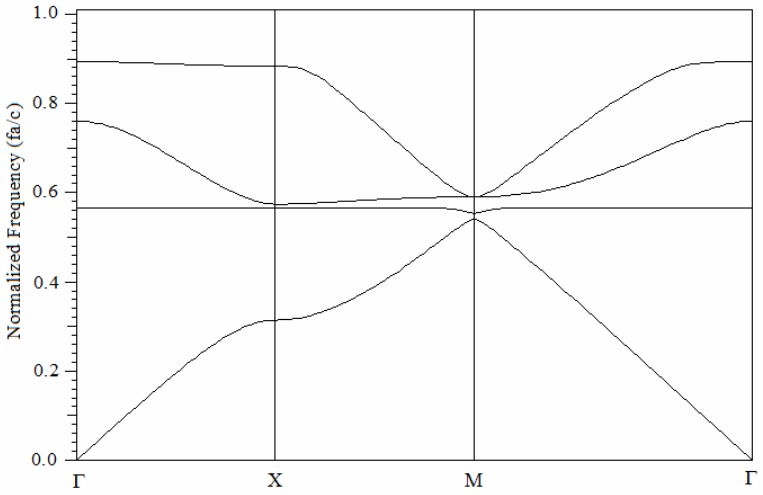

Fig.4: Band diagram (H-polarization) for the PhCs with metallic (Ag) nanoshelled cylinders. The coated cylinders with core radius of 225nm and shell thickness of 37.5nm are arranged on a square lattice with lattice constant a = 750nm.

Intensive numerical investigations have shown that for most of the metals, no matter whether measured data or realistic Drude-like fitting models are used, no flat band will appear in the structure if the lattice constant is comparable to the operating wavelength. This can be assigned to the material losses in the MPhC structures where the modes are already attenuated along such characteristic length scale. However, the surface plasmon behaviors are still observable in the structure as displayed in Figure 5 by the field distribution of the MPhC lattice's eigenmodes.

The recently demonstrated plasmonic waveguide devices are mainly based on linear arrays of coupled metallic particles [36]. As we know, light can propagate in such structure mainly because of surface plasmon resonances and the strong coupling associated between nanoparticles. (Note that the propagation length in such plasmonic waveguide is also limited by the losses in the metal). Referring to the plasmonic waveguide and a new idea then comes up for the MPhCs:

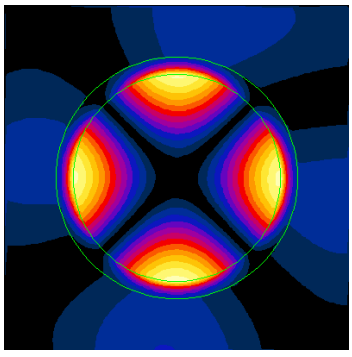

Fig.5: The H-field distribution of the fourth order eigenmode located at the Γ point in the first Brillouin zone for the MPhC under investigation.

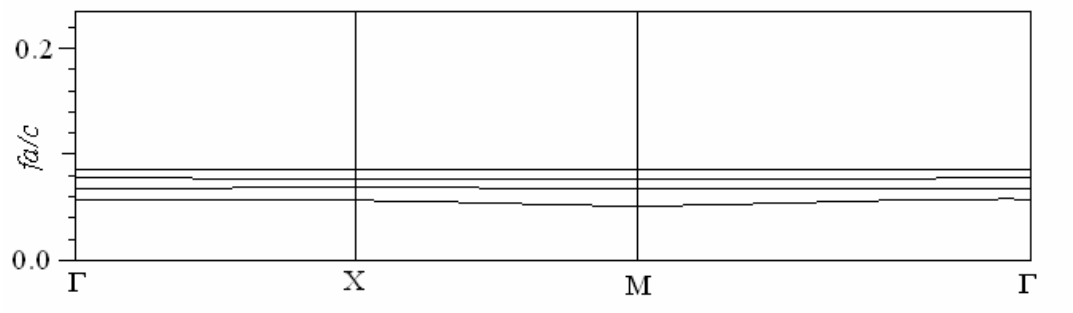

Fig.6: Band diagram (H-polarization) for a PhC with metallic (Ag) nanoshelled cylinders arranged on a square lattice with lattice constant a = 75nm. The core radius of the coated cylinder is 25.8nm and the shell thickness is 0.55nm. Note that this diagram is not complete: infinitely many additional higher modes may be found near the reduced frequency $fa/c \sim 0$, where the resonance condition is also satisfied.

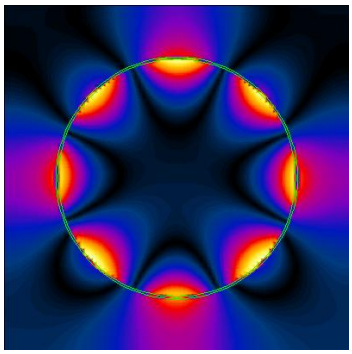

Fig.7: The H-field distribution of the fourth eigenmode located at Γ point in the first Brillouin zone in the MPhC with a = 75nm.

In the MPhCs, if the cylinders are put more closely, then the lattice constant is reduced to much less than the operating wavelength. As a result of the strong interaction the coupling between cylinders is therefore enhanced. In addition, the reduced metallic volume in the nanoshelled cylindrical MPhC also means a substantial reduction in material losses, which could enhance the mode propagation in the structure as well. In order to test the idea, the lattice constant a of the underlying structure shown in Fig.4 are shrinked by a factor of ten (a = 75nm) and the band structure is then recalculated (for H-polarization). The core radius r_1 is selected as 25.8 nm and with the shell thickness 0.55nm. The calculated band diagram is shown in Fig.6 and we can see that the flat bands appeared in the structure as we expected. This means that in the metal-shelled MPhCs, the flat bands are possible when the lattice constant of the MPhCs is selected to be much less than the operating wavelength while keeping the metallic volume as small as possible. It can be explained as that the flat bands in the metal-shelled MPhCs originate from the surface plasmon resonances, and the mode energy transport in the structure relies on near field coupling between surface plasmon modes of neighboring particles [36]. This would make sense because the flat band modes in MPhCs are associated with low group velocities, which have already discharged into very interesting applications [37]. Accordingly, the surface plasmon behaviors are verified by examining the eigenfield of the modes in certain lattices as shown in Fig.7. The displayed mode patterns indicate that the interaction between neighboring nanoparticles can produce mixing and splitting of these dipolar modes. Typically, this type of

hybridization of the plasmon excitations is essentially the result of a strong coupling of plasmon states in the inner and outer metal shells and it appears to be very sensitive to the thickness of the separating dielectric layer. Then the metal-shelled MPhC structure should be carefully designed and optimized to obtain corresponding optical responses.
In fact, because of the strong coupling between nanoparticles, the structure we calculated here can be used where locally strong fields are desirable. One possible application of the structure is the substrate of SERS, where the molecules under detected are put at the locations where the field is stronger for some specific wavelength. Our calculation reveals that field enhancement factors larger than 100 are possible under resonance condition.

IV. CONCLUSIONS

We have applied a rigorous analysis to investigate both single metallic nanoshelled cylinder in the vacuum, and the MPhC structure made by the metallic nanoshelled cylinder arranged on a square lattice and embedded in air as background medium. An accurate material model was used to explore the aforementioned nanostructures. Plasmon wavelengths larger than 8μm are predicted via numerical simulation for cylindrical nanoshell structure. We have shown that the plasmons exhibited by the metallic nanoparticles could hybridize in a photonic crystal setting when the particles are close enough to each other, and this produces new plasmon-like modes whose frequency can be tuned by changing the lattice constant and the metallic shell thickness. In the case of MPhCs, we verified this by computing the band structure of the MPhCs for lattice constants much less than the operating wavelength. The emergent flat bands in such MPhCs suggests potential applications e.g. for sensing based on changes in the plasmon frequency with small variations in the structure or the environment. Enhanced sensitivities are expected here because of the high amount of surfaces in the MPhC topology in conjunction with light fields that are confined just to those surfaces.

REFERENCES

1. Daniel. L. Feldheim, Colby A. Forr. Jr, *Metal nanoparticles: Synthesis, Characterization, and Applications,* Marcel Dekker Inc., New York, 2002.
2. Suchita Kalele, S. W. Gosavi, J. Urban and S. K. Kulkarni, *Current Science*, **91** (8), 1038-1052, (2006).
3. A. Dahlin, M. Zach, T. Rindzevicius, M, Kall, D. S. Sutherland, F. Hook, *J. Am. Chem. Soc.,* **127**, 5043-5048, (2005).
4. E. Hutter, J. H. Fendler, *Adv. Mater.*, **16**, 1685-1706, (2004).
5. S. A. Maier, H, A. Atwater, *J. Appl. Phys.*, **98**, 011101 (2005).
6. A. J. Haes, R. P. Van Duyne, *Anal. Bioanal. Chem.*, **379**, 920-930, (2004).
7. J. B. Jackson, N. J. Halas, *Proc. Natl. Acad. Sci. USA*, **101**, 17930-17935, (2004).
8. C. L. Haynes, A. D. McFarland, R. P. Van Duyne, *Anal. Chem*., **77**, 338A-346A, (2005).
9. A. H. Haes, C. L. Haynes, A. D. McFarland, G. C. Schatz, R. P. Van Duyne, S. L. Zou, *MRS Bulletin*, **30**, 368-375, (2005).
10. A. D. McFarland, M. A. Young, J. A. Dieringer, R. P. Van Duyne, *J. Phys. Chem. B*, **109**, 11279-11285, (2005).
11. Xudong Cui, Weihua Zhang, Boon-Siang Yeo, Renato Zenobi, Christian Hafner, Daniel Erni, *Opt. Express*, **15**, 8309-8316, (2007).
12. A. L. Stepanov, J. R. Krenn, H. Ditlbacher, A. Hohenau, A. Drezet, B. Steinberger A. Leitner, F. R. Aussenegg, *Opt.*

Lett., **30**, 1524-1526, (2005).
13. H. Ditlbacher, J. R. Krenn, A. Leitner, F. R. Aussenegg, *Opt. Lett.*, **29**, 1408-1410, (2004).
14. M. Salerno, J. R. Krenn, B. Lamprecht, G. Schider, H. Diltbacher, N. Felidj, A. Leitner, F. R. Aussenegg, *Opto Electronics Rev.*, **10**, 217-224, (2002).
15. William L. Barnes, *Nature Materials*, **3**, 588-589, (2004).
16. R. D. Averitt, D. Sarkar, N. J. Halas, *Phys. Rev. Lett*., **78**, 4217-4220 (1997).
17. S. J. Oldenburg, R. D. Averitt, S. L. Westcott, N. J. Halas, *Chem. Phys. Lett*., **288**, 243-247, (1998).
18. C. F. Bohren, D. R. Huffman, *Absorption and Scattering of light by small particles*, Wiley, New York, 1983.
19. B. T. Drainer, P. J. Flatau, *J. Opt. Soc. Am. A*, **11**, 1491-1499, (1994).
20. http://alphard.ethz.ch/max-1.
21. A. Taflove, *Computational Electrodynamics: The Finite Difference Time Domain Method*, Boston, Artech House, 1995.
22. A. Plaks, I. Tsukerman, G. Freidman, B. Yellen, IEEE Trans. On Magnetics, 39, 1436-1439, (2003).
23. Ch.Hafner, *Post modern electromagnetics using intelligent Maxwell solver*, John-Wiley & Sons, 1999.
24. J. A. A. J. Perenboom, P. Wyder, F. Meier, *Phys. Rev. B*, **7**, 173 (1981).
25. C. Kittel, *Introduction to Solid State Physics*, Wiley, New York, 1976.
26. A. E. Neeves, M. H. Birnboim, *J. Opt. Soc. Am. B*., **6**, 787-796, (1989).
27. P. B. Johnson, R. W. Christy, *Phys. Rev. B.,* **6**, 4370, (1972).
28. Ch. Hafner, *J. Comp. Theo. Nanosci.*, **2**, 88-98, (2005).
29. S. L. Westcott, J. B. Jackson, C. Radloff, N. J. Halas, *Phys. Rev. B*, **66**, 155431, (2002).
30. E. Yablonovitch, *Phys. Rev. Lett.*, **58**, 2059, (1987).
31. D. R. Smith, W. J. Padilla, D. C. Vier, S. C. Nemat-Nasser, S. Schultz, *Phys. Rev. Lett.*, **84**, 4184, (2000).
32. Nick N. Lepeshkin, Aron Schweinsberg, Giovanni Piredda et al., *Phys. Rev. Lett.,* **93**, 123902, (2004).
33. Ch. Hafner, Cui Xudong, R. Vahldieck, *J. Comp. Theor. Nanosci,* **2**, 240-250, (2005).
34. Cui Xudong, Christian Hafner, Ruediger Vahldieck, Opt. Express, 13, 6175-6180, (2005).
35. K. Sakoda, N. Kawai, T. Ito, *Phys. Rev. B*, **64**, 045116 (2001).
36. Stefan A. Maier, Pieter G. Kik, Harry A. Atwater, Appl. Phys. Lett., 81, 1714-1716, (2002).
37. K. Sakoda, *Optical Properties of Photonic Crystals*, Springer-Verlag, Berlin, 2001.